

Cluster-in-jellium model and icosahedral ordering tendencies in liquid Al alloys

Y. X. Yao, C. Z. Wang, and K. M. Ho

Ames Laboratory-U.S. DOE and Department of Physics and Astronomy, Iowa State University, Ames, Iowa 50011, USA

(Received 12 August 2007; revised manuscript received 23 October 2007; published 29 November 2007)

A jellium-passivated cluster model is developed to study the energetics of short-range ordering in supercooled liquid and glass systems. Calculations for single atoms embedded in jellium yield results in good agreement with bulk values for the cohesive energy, atomic volume, as well as angular-momentum-projected electronic density of states. The energy difference between icosahedral clusters and fcc embryos in jellium is found to correlate with the glass-forming ability of liquid Al alloys. The model will be useful for studying the short-range order tendency with minor chemical additions in metallic glass formation, without the use of large unit cell calculations.

DOI: 10.1103/PhysRevB.76.174209

PACS number(s): 61.25.Mv, 61.43.Fs, 61.46.Bc, 71.15.Mb

I. INTRODUCTION

Short-range order in undercooled metallic liquids plays an essential role in glass formation in these systems. Many experiments using scattering and absorption techniques have been employed to study this problem. Meanwhile, computer simulations have also been widely used to track the atomic structure evolution in liquid metallic alloys. As a result of these efforts, local cluster structures for some model binary systems have been demonstrated.¹ Experimentally, it has been observed that the glass-forming ability of various systems is quite sensitive to their chemical compositions. This implies that the energetics and packing of local clusters may be dominant factors in the glass-formation process. With the fast development of computational capabilities, calculations of isolated clusters are now a mature procedure. However, the energies and local structures of clusters in supercooled liquid or glass could be very different from isolated clusters due to the different environments. For instance, the structures of Si clusters with hydrogen passivation are tremendously different from those of free Si clusters.² In fact, the passivation of metallic clusters is still an unresolved problem.³

In this paper, we use a mean-field approach to calculate the energetics of local clusters in supercooled metallic liquid or glass by studying clusters embedded in an effective jellium background. There are many studies on bonding properties of elemental metals using jellium approaches.⁴⁻⁹ The difference of our present approach from previous jellium studies (e.g., Puska's atom-in-jellium model^{4,9}) is that, in our embedding scheme, we consider a volume around the atom or cluster where the jellium background is excluded. The size of the excluded volume is determined by minimizing the total system energy. Our jellium-passivation calculations yield good agreement with the cohesive energies and atomic volumes obtained from bulk calculation. The site- and angular-momentum-projected densities of states (PDOS) from the jellium passivation approach are also in good agreement with bulk results. Calculations for clusters with increasing size show that jellium passivation gives good estimates for the bulk limit of large clusters. We believe that the jellium-passivation approach will be a promising method to provide useful energetic information about the glass-formation tendency of various liquid metal systems. It may

be further improved for incorporation in local molecular dynamics simulations which can concentrate on the evolution of short-range or medium-range order in such systems while maintaining a reasonable simulation size.

II. MODEL AND FORMALISM

A local cluster in supercooled liquid or glass is modeled as a cluster surrounded by jellium corresponding to the liquid metal environment in a mean-field approach, as illustrated in Fig. 1(a). The central circle represents the cluster, surrounded by an empty space representing the optimized volume occupied by the cluster. The most outside region is the effective jellium background representing the electron sea coming from the liquid metal environment. Following the notations of the classic paper by Ihm *et al.*,¹⁰ the total energy for the jellium-passivated cluster under density functional theory pseudopotential framework in Rydberg units can be expressed as¹¹

$$E_{tot} = T + V + \int E_{xc}(\mathbf{r}) d^3\mathbf{r} - m_0 \epsilon_{jel}(n_0), \quad (1)$$

where T is the kinetic energy of the whole system,

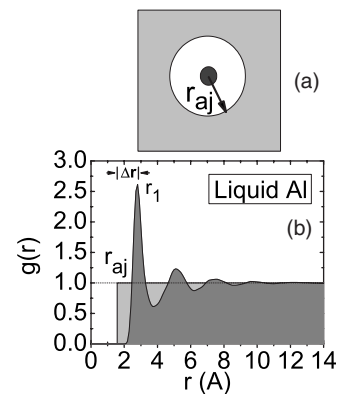


FIG. 1. (a) Schematic representation of the cluster-in-jellium model. (b) Gray area: pair distribution function of liquid aluminum; light gray area: uniform jellium as an approximation for the liquid metallic environment.

$$T = \sum_n \int f_n \psi_n^*(\mathbf{r}) (-\nabla^2) \psi_n(\mathbf{r}) d^3\mathbf{r}, \quad (2)$$

V is the electrostatic potential energy,

$$\begin{aligned} V = & \sum_{n,i,l} \int f_n \psi_n^*(\mathbf{r}) U_{ps,l}(\mathbf{r}-\mathbf{R}_i) \hat{P}_l \psi_n(\mathbf{r}) d^3\mathbf{r} \\ & + \frac{1}{2} \int \int \frac{2\rho(\mathbf{r})\rho(\mathbf{r}')}{|\mathbf{r}-\mathbf{r}'|} d^3\mathbf{r} d^3\mathbf{r}' + \int v(\mathbf{r}) n_e(\mathbf{r}) d^3\mathbf{r} \\ & + \frac{1}{2} \sum_{i,j} \frac{2Z^2}{|\mathbf{R}_i-\mathbf{R}_j|} + \sum_i \int \frac{2Zn_b(\mathbf{r})}{|\mathbf{r}-\mathbf{R}_i|} d^3\mathbf{r}, \quad (3) \end{aligned}$$

and E_{xc} is the exchange-correlation energy. Here, m_0 is the total number of electrons contributed by the jellium, $\epsilon_{jel}(n_0)$ gives the energy per electron in bulk jellium with density of n_0 , which can be expressed analytically,¹² and n is the index for both wave vector \mathbf{k} and band. Indices i and j run over all the atomic lattice sites. $\sum_l U_{ps,l}(\mathbf{r}-\mathbf{R}_\mu) \hat{P}_l$ is angular-momentum-dependent pseudopotentials, where \hat{P}_l is the projection operator on angular momentum l . Here, f_n specifies the occupancy of quantum state n . Moreover, $v(\mathbf{r})=v_0\gamma(\mathbf{r})$, where v_0 is the constant electron chemical potential shift for the jellium background and $\gamma(\mathbf{r})$ is a step function which is one in jellium and zero outside. Furthermore, $n_b(\mathbf{r})=n_b^0\gamma(\mathbf{r})$, n_b^0 is the positive background charge density and $n_b(\mathbf{r})$ is position dependent because of the excluded volume in our model. $n_e(\mathbf{r})=\sum_n f_n \psi_n^*(\mathbf{r}) \psi_n(\mathbf{r})$ is the total electron density including the contributions from the cluster and jellium, and $\rho(\mathbf{r})=n_e(\mathbf{r})-n_b(\mathbf{r})$. The first term in Eq. (3) describes the interaction between total electron n_e and ion cores. For simplicity, the formalism is given for a single-element cluster. It can be easily generalized to multielement clusters. Assuming that the positive background charge does not overlap with the pseudopotential's core region where the Coulomb potential is smoothed, the expression for V can be written as

$$\begin{aligned} V = & \int V_{ion+jel}(\mathbf{r}) n_e(\mathbf{r}) d^3\mathbf{r} \\ & + \sum_{n,i,l} \int f_n \psi_n^*(\mathbf{r}) U'_{ps,l}(\mathbf{r}-\mathbf{R}_i) \hat{P}_l \psi_n(\mathbf{r}) d^3\mathbf{r} \\ & + \frac{1}{2} \int \int \frac{2\rho(\mathbf{r})\rho(\mathbf{r}')}{|\mathbf{r}-\mathbf{r}'|} d^3\mathbf{r} d^3\mathbf{r}' - \int V_{ion}^{loc}(\mathbf{r}) n_b(\mathbf{r}) d^3\mathbf{r} \\ & + \frac{1}{2} \sum_{i,j} \frac{2Z^2}{|\mathbf{R}_i-\mathbf{R}_j|}, \quad (4) \end{aligned}$$

where $V_{ion+jel}=V_{ion}^{loc}+v(\mathbf{r})$, V_{ion}^{loc} is the pure local pseudopotential, and $U'_{ps,l}$ denotes the angular-momentum-dependent nonlocal part of the pseudopotential. The corresponding one-particle Schrödinger equation is

$$\begin{aligned} & \left(-\nabla^2 + \sum_{i,l} U'_{ps,l}(\mathbf{r}-\mathbf{R}_i) \hat{P}_l + V_{ion+jel}(\mathbf{r}) \right. \\ & \left. + \int \frac{2\rho^{in}(\mathbf{r}')}{|\mathbf{r}-\mathbf{r}'|} d^3\mathbf{r}' + \mu_{xc}^{in}(\mathbf{r}) \right) \psi_n(\mathbf{r}) = \epsilon_n \psi_n(\mathbf{r}), \quad (5) \end{aligned}$$

where μ_{xc} is the exchange-correlation potential. Based on the solution of the Schrödinger equation, the total energy can be expressed as a variational functional of the output electron density only,¹³

$$\begin{aligned} E_{tot} = & \sum_n f_n \epsilon_n - \int \frac{2\rho^{in}(\mathbf{r})n_e^{out}(\mathbf{r})}{|\mathbf{r}-\mathbf{r}'|} d^3\mathbf{r} d^3\mathbf{r}' - \int \mu_{xc}^{in} n_e^{out}(\mathbf{r}) d^3\mathbf{r} \\ & + \frac{1}{2} \int \frac{2\rho^{out}(\mathbf{r})\rho^{out}(\mathbf{r}')}{|\mathbf{r}-\mathbf{r}'|} d^3\mathbf{r} d^3\mathbf{r}' + \int \epsilon_{xc}^{out}(\mathbf{r}) n_e^{out}(\mathbf{r}) d^3\mathbf{r} \\ & - \int V_{ion,loc}(\mathbf{r}) n_b(\mathbf{r}) d^3\mathbf{r} + \frac{1}{2} \sum_{i,j} \frac{2Z^2}{|\mathbf{R}_i-\mathbf{R}_j|} - m_0 \epsilon_{jel}(n_0). \quad (6) \end{aligned}$$

In the momentum space representation, the total energy is

$$\begin{aligned} E_{tot} = & \sum_n \epsilon_n f_n + \Omega \left(- \sum_{\mathbf{G}} V_{Coulomb}^{in}(\mathbf{G}) n_e^{out}(\mathbf{G}) \right. \\ & - \sum_{\mathbf{G}} \mu_{xc}^{in}(\mathbf{G}) n_e^{out}(\mathbf{G}) + \frac{1}{2} \sum_{\mathbf{G}} V_{Coulomb}^{out}(\mathbf{G}) \rho^{out}(\mathbf{G}) \\ & \left. + \sum_{\mathbf{G}} \epsilon_{xc}^{out}(\mathbf{G}) n_e^{out}(\mathbf{G}) - \sum_{\mathbf{G}} V_{ion,loc}(\mathbf{G}) n_b(\mathbf{G}) \right) \\ & + \frac{1}{2} \sum_{i,j} \frac{2Z^2}{|\mathbf{R}_i-\mathbf{R}_j|} - m_0 \epsilon_{jel}(n_0), \quad (7) \end{aligned}$$

where $V_{Coulomb}=8\pi\rho(\mathbf{G})/\mathbf{G}^2$. By the same argument as Ihm *et al.*,¹⁰ finally, the total energy per unit cell can be expressed as

$$\begin{aligned} E_{tot,cell} = & \frac{1}{N} \sum_n \epsilon_n f_n + \Omega_{cell} \left(- \sum_{\mathbf{G}} V_{Coulomb}^{in}(\mathbf{G}) n_e^{out}(\mathbf{G}) \right. \\ & - \sum_{\mathbf{G}} \mu_{xc}^{in}(\mathbf{G}) n_e^{out}(\mathbf{G}) + \frac{1}{2} \sum_{\mathbf{G}} V_{Coulomb}^{out}(\mathbf{G}) \rho^{out}(\mathbf{G}) \\ & \left. + \sum_{\mathbf{G}} \epsilon_{xc}^{out}(\mathbf{G}) n_e^{out}(\mathbf{G}) - \sum_{\mathbf{G}} V_{ion,loc}(\mathbf{G}) n_b(\mathbf{G}) \right) \\ & + \alpha_1 Z + \gamma_{Ewald} - \frac{m_0}{N} \epsilon_{jel}(n_0), \quad (8) \end{aligned}$$

where V' indicates the term with $G=0$ set to be zero, which is equivalent to a constant shift of the potential.

The above formalism is incorporated into our pseudopotential mixed-basis code.^{14,15} Norm-conserving pseudopotentials are generated with the Troullier-Martins method.¹⁶ For transition metals, the localized character of d electrons can be efficiently expressed by including truncated atomic

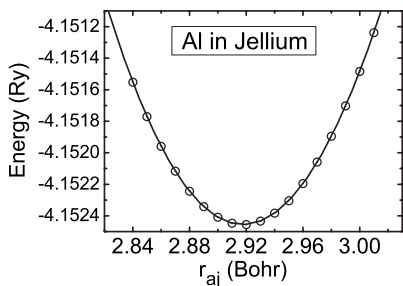


FIG. 2. The total energy of Al atom passivated by jellium as a function of the distance between the atom and the jellium boundary r_{aj} .

pseudo-wave-functions in the basis set in addition to plane waves. The exchange-correlation potential is based on the generalized gradient corrections parametrized by Perdew-Burke-Ernzerhof.¹⁷ The calculations are done in the supercell approach with a cubic unit cell with length of 20 bohr. The plane wave cutoff energy is 20 Ry. A Gaussian smearing width of 0.06 eV is used for the Brillouin zone integration on a $6 \times 6 \times 6$ Monkhorst-Pack grid. The jellium boundary is smoothed by Fermi smearing with a width of 0.05 bohr to remove high Fourier components.

III. RESULTS AND DISCUSSION

A. Single atom embedded in jellium

The excluded volume occupied by an atom in our model can be understood by considering the pair distribution function $g(r)$ in liquid or glass. Figure 1(b) shows a typical pair distribution function of liquid Al (gray area), which describes the average environment of an Al atom in the liquid. In a mean-field approach, the environment can be approximated as an effective jellium (light gray area). The optimized atom-jellium spacing r_{aj}^o must be smaller than the first peak position of the pair distribution function r_1 from mass conservation.

The jellium density parameter could be obtained from the average interstitial electron density from local-density approximation calculations.¹⁸ It was known that bare jellium model failed qualitatively to describe the energetics of met-

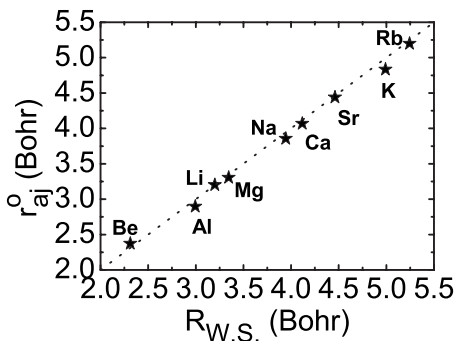


FIG. 3. Correlation between the optimized atom-jellium distance r_{aj}^o and the Wigner-Seitz radius R_{WS} for nine simple metals.

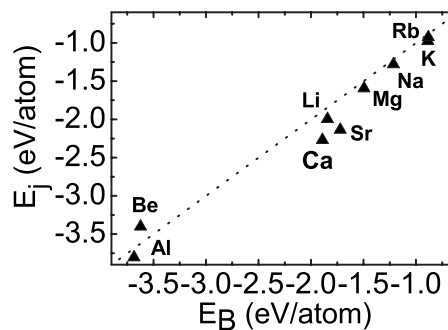


FIG. 4. Correlation between the cohesive energies of the simple metals from the jellium-passivation approach E_j and those from bulk calculation E_B .

als; e.g., the predicted surface energy could be negative for large electron density.¹⁹ Utreras Diaz and Shore showed that this shortcoming of the jellium model can be corrected by adding a constant shift v_0 to the electron potential of the jellium background.⁵ We follow the simple procedure outlined in Refs. 7 and 8 to estimate v_0 from jellium density, $v_0 = -n_0 [\partial \epsilon_{el} / \partial n]_{n_0}$. In the case of aluminum, using the chemical potential shift of -0.17 Ry from Ref. 8, we obtained 2.92 bohr for the optimized atom-jellium distance. This is fairly close to the Wigner-Seitz radius of bulk Al (2.99 bohr). Figure 2 shows a typical result of the total energy of an Al atom embedded in jellium with respect to the atom-jellium spacing r_{aj} , which is well fitted by a third order polynomial function. A good correlation between r_{aj}^o and Wigner-Seitz radius R_{WS} , for nine simple metals is shown in Fig. 3. The cohesive energies of the simple metals from the jellium-passivation approach E_j are also compared with the bulk results E_B , as shown in Fig. 4. A similar trend was observed from another jellium approach.^{8,9} Such good agreement suggests that the jellium background is a good approximation of the bulk environment for simple metals.

In order to gain deeper insight into jellium passivation, we also compared the angular-momentum-projected density of states (DOS) of Al in jellium-passivation approach with the bulk result, as shown in Fig. 5. 2.99 bohr is selected to be the radius of the atomic sphere for the integration of the wave functions and yields 3.0 electrons in both cases. The fairly

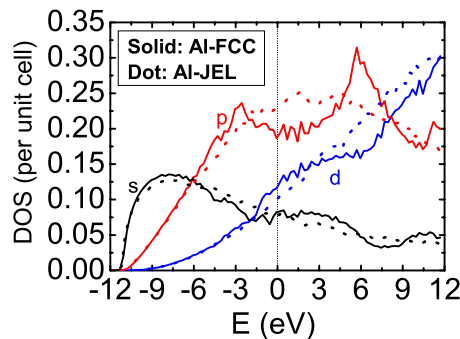


FIG. 5. (Color online) Angular-momentum-projected density of states (PDOS) for Al in fcc crystal structure (solid line) and embedded in jellium (dots).

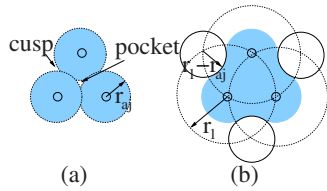


FIG. 6. (Color online) Schematic illustration of the jellium boundaries for an Al trimer. (a) Simplest generalization of single atom-in-jellium treatment results in pockets and cusps. (b) Push-pull strategy for jellium boundary construction. Shaded (light blue) area corresponds to the region where jellium is excluded.

good match reveals the essential physical justification of jellium passivation for Al.

B. Clusters embedded in jellium

To generalize the treatment of single atom in jellium to cluster in jellium, we need to determine the shape and position of the jellium boundary. In the case of a single atom, the shape of the jellium boundary is taken to be spherical. In our calculations, we want the jellium to represent the embedding environment and want the jellium background to be kept away from the “inside” region of the cluster. The simplest generalization of the treatment for single atom in jellium is to empty a spherical region with optimized atom-jellium radius centered at each atom in the cluster. However, because the volume per spherical region is similar to the volume per atom and there are significant overlaps in the spheres centered on different atoms in the cluster, this approach does not remove enough space from inside the cluster and allows some pockets of jellium to persist inside the cluster, as shown in Fig. 6(a). Also, the resulting boundary exhibits sharp cusps at the spherical intersections, leading to high Fourier components not easy to remove. We found an approach which works better to follow a “push-pull” strategy, which is physically motivated by the pair distribution function in Fig. 1(b); jellium is first pushed outward to a nearest-neighbor distance [corresponding to r_1 , the nearest-neighbor peak position in $g(r)$] from each atom in the cluster and then pulled inward $\Delta r = r_1 - r_{aj}$ from the initial boundary, as shown in Fig. 6(b). The advantages of the push-pull strategy are (a) smooth jellium boundaries good for Fourier transform, (b) no jellium inside the cluster, and (c) jellium boundary reflects the morphology of the cluster’s surface which is desired physically.

Fivefold icosahedral local order has been linked with the short-range and medium-range orders in metallic glass system.¹ Local icosahedral clusters may serve as competitors against possible nuclei for crystallization. Thus, the interesting questions are the relative stability of the icosahedral cluster and a crystal nuclei inside an undercooled liquid metal system and how well it correlates with the glass-forming ability (GFA) of the metallic liquid. Here, we choose a series of Al-X ($X = \text{Na, K, Mg, Ca, Sr, Al, Si, Ge, Sn, Ni, Mo, Zn, Zr, Pt, Pd, Cu, Ag, and Au}$) binary alloys and examine the energy difference of local icosahedral clusters and fcc embryos in a jellium environment approximating liquid Al. The

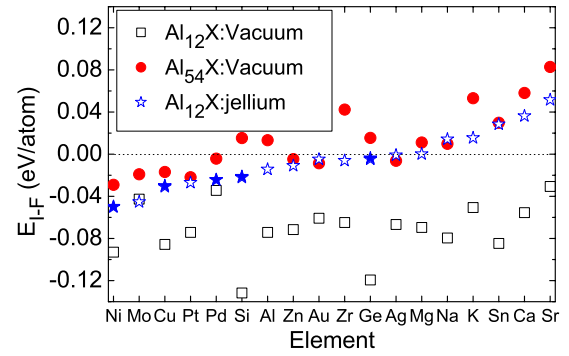


FIG. 7. (Color online) Energy difference between icosahedral clusters and fcc fragments of Al with central atom replaced by X (Ni, Mo, ...) with jellium passivation, which is a good estimate of the bulk limit of nonisolated clusters as shown by the trend in the energy differences for free clusters with one shell of Al ($\text{Al}_{12}+X$) and two shells of Al ($\text{Al}_{54}+X$). Solid star represents the system where coexistent amorphous and crystalline phases have been observed experimentally.

local icosahedral cluster for Al-X liquid is an Al_{13} icosahedral cluster with central atom replaced by a solute atom X. Similarly, the fcc embryo is a pure solvent Al_{13} fcc fragment with central atom replaced by a solute atom X. Figure 7 shows the energy difference between the icosahedral clusters and fcc fragments of Al-X liquid with jellium passivation. The energy differences for free clusters with one shell of Al ($\text{Al}_{12}+X$) and two shells of Al ($\text{Al}_{54}+X$) are also shown. Spin polarization effects are found to be negligible for the systems studied in this paper. Good correlation exists between the jellium-passivation results, $E_{I-F,jel}$, and those by adding one more shell of Al atoms, $E_{I-F,2-shell}$, as shown in Fig. 8. The free cluster calculation results show that the behavior of the energy difference approaches the cluster-in-jellium results as the free clusters increase in size. This suggests that the jellium-passivated result is a good estimate of the energy behavior of the cluster inside a liquid metal system.

Looking at the trend of the energy differences for the various choices of X, we found a good correlation with the size of the center atom (Fig. 9). This suggests that smaller

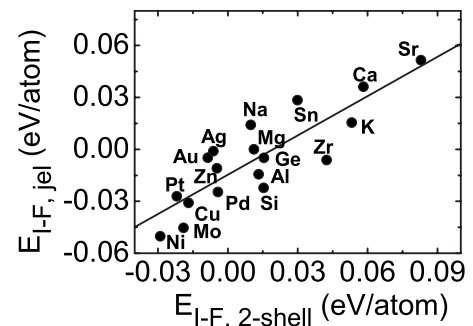


FIG. 8. Correlation between the energy differences of icosahedral cluster and fcc fragment in jellium-passivation approach ($E_{I-F,jel}$) and those by adding one more shell of Al atoms ($E_{I-F,2-shell}$). The solid line is a linear least squares fitting of the data.

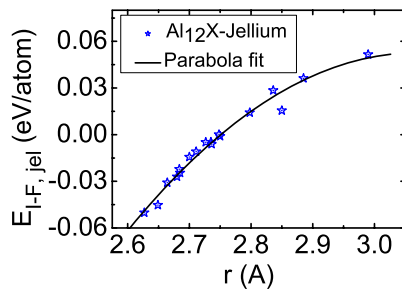


FIG. 9. (Color online) The energy difference as a function of the distance between the central atom X and outer shell Al atom.

atoms allow for a more efficient packing for the icosahedral cluster²⁰ relative to the fcc embryo structure. Experimentally, coexistent amorphous and crystalline phases have been observed in Al-Si,²¹ Al-Ge,²² Al-Cu,²³ Al-Ni,²⁴ and Al-Pd,²⁵ corresponding to a region of negative $E_{I-F,jel}$ in Fig. 7. Thus, the energy difference between icosahedral cluster and fcc embryos with jellium passivation may serve as an indication for GFA of Al-rich liquid metallic alloys.

In many cases, the glass transformation of liquid metal alloy systems is very sensitive to the addition of small amounts of impurity atoms.²⁶ A fundamental understanding of the role of the small amount of added material is critical for a successful theory of glass transformation. Our cluster-in-jellium model could be further developed to study the

effects of low-concentration impurity atoms on the energetics, structures, and dynamical behavior of important local clusters without the use of large unit cell calculations.

IV. CONCLUSIONS

We have used a model of clusters embedded in jellium to study short-range ordering in supercooled liquid and glass systems in a mean-field approach. The model was first verified by the good agreement between the single atom-in-jellium results and those from bulk calculations. The PDOS of Al atom embedded in jellium matches very well with bulk result. Application of the model to Al- X metallic liquid shows that cluster passivated by jellium is a reasonable estimate for the bulk limit. Furthermore, the energy differences between icosahedral clusters and fcc embryos are related with the GFA of the metallic liquids. The model may be further developed to study a critical issue of glass formation—the effect of minor addition of other chemical elements on the glass behavior of liquid metal alloy system.

ACKNOWLEDGMENTS

Ames Laboratory is operated for the U.S. Department of Energy by Iowa State University under Contract No. W-7405-Eng-82. This work was supported by the Director for Energy Research, Office of Basic Energy Sciences.

-
- ¹W. Sheng, W. K. Luo, F. M. Alamgir, J. M. Bai, and E. Ma, *Nature (London)* **439**, 419 (2006).
- ²Mingsheng Tang, C. Z. Wang, W. C. Lu, and K. M. Ho, *Phys. Rev. B* **74**, 195413 (2006).
- ³I. L. Garzón, C. Rovira, K. Michaelian, M. R. Beltrán, P. Ordejón, J. Junquera, D. Sánchez-Portal, E. Artacho, and J. M. Soler, *Phys. Rev. Lett.* **85**, 5250 (2000).
- ⁴M. J. Puska, R. M. Nieminen, and M. Manninen, *Phys. Rev. B* **24**, 3037 (1981).
- ⁵C. A. Utreras Diaz and H. B. Shore, *Phys. Rev. Lett.* **53**, 2335 (1984).
- ⁶J. P. Perdew, H. Q. Tran, and E. D. Smith, *Phys. Rev. B* **42**, 11627 (1990).
- ⁷H. B. Shore and J. H. Rose, *Phys. Rev. Lett.* **66**, 2519 (1991).
- ⁸J. H. Rose and H. B. Shore, *Phys. Rev. B* **43**, 11605 (1991).
- ⁹M. J. Puska and R. M. Nieminen, *Phys. Rev. B* **43**, 12221 (1991).
- ¹⁰J. Ihm, A. Zunger, and M. L. Cohen, *J. Phys. C* **12**, 4409 (1979).
- ¹¹ $\hbar = 2m_e = e^2/2 = 1$ from Gaussian units to Rydberg units
- ¹²*A Primer in Density Functional Theory*, edited by C. Fiolhais, F. Nogueira, and M. Marques, Lecture Notes in Physics Vol. 620 (Springer, Berlin, 2003), pp. 1–55.
- ¹³W. E. Pickett, *Comput. Phys. Rep.* **9**, 115 (1989).
- ¹⁴S. G. Louie, K.-M. Ho, and M. L. Cohen, *Phys. Rev. B* **19**, 1774 (1979).
- ¹⁵K. M. Ho, C. Elsässer, C. T. Chan, and M. Fähnle, *J. Phys.: Condens. Matter* **4**, 5189 (1992).
- ¹⁶N. Troullier and J. L. Martins, *Phys. Rev. B* **43**, 1993 (1991).
- ¹⁷J. P. Perdew, K. Burke, and M. Ernzerhof, *Phys. Rev. Lett.* **77**, 3865 (1996).
- ¹⁸V. L. Moruzzi, J. F. Janak, and A. R. Williams, *Calculated Electronic Properties of Metals* (Pergamon, New York, 1978).
- ¹⁹N. D. Lang and W. Kohn, *Phys. Rev. B* **1**, 4555 (1970).
- ²⁰C. Ashman, S. N. Khanna, Feng Liu, P. Jena, T. Kaplan, and M. Mostoller, *Phys. Rev. B* **55**, 15868 (1997).
- ²¹P. Predecki, B. C. Giessen, and N. J. Grant, *Trans. Metall. Soc. AIME* **233**, 1438 (1965).
- ²²P. Ramachandrarao, M. Laridjani, and R. W. Cahn, *Z. Metallkd.* **63**, 43 (1972).
- ²³H. A. Davies and J. B. Hull, *Scr. Metall.* **6**, 241 (1972).
- ²⁴K. Chattopadhyay, R. Ramachandrarao, S. Lele, and T. R. Anantharaman, in *Proceedings of the Second International Conference on Rapidly Quenched Metals*, edited by N. J. Grant and B. C. Giessen (MIT, Massachusetts, 1976) Sec. I, p. 157.
- ²⁵G. V. S. Sastry, C. Suryanarayana, O. N. Srivastava, and H. A. Davies, *Trans. Indian Inst. Met.* **31**, 292 (1978).
- ²⁶Wei Hua Wang, *Prog. Mater. Sci.* **52**, 540 (2007).